ON THE LATERAL FORCE DISTRIBUTION AMONG STRUCTURAL WALLS IN MULTISTOREY BUILDINGS

Avigdor Rutenberg[1] and Edward Leibovich[2]

ABSTRACT

The seismic behaviour of regular multistorey structures supported laterally by a number of reinforced concrete cantilever walls with markedly different lengths is addressed. It is shown that the shear force distribution among the walls is strongly affected by the different yield displacement levels of the walls. The share of the shear force carried by the shorter walls is shown to be larger than their share in the bending moment. The dynamic amplification of the shear forces due to multi-mode effects and the implications for capacity design are noted. Numerical examples illustrate the problem.

INTRODUCTION

The static procedures used by practitioners and researchers for code-based seismic design of reinforced concrete structures have been criticized during the last decade as not being sufficiently realistic. Paulay [1] states: "existing code recommendations, expressed only in terms of the properties of elastic structures, are largely irrelevant when the design needs to be based on ductile system behaviour" Although directed towards asymmetric structures this criticism is equally pertinent to symmetric ones, and it would be interesting to study its implications on the lateral force distribution among structural walls in multistorey buildings.

The thrust of Paulay's criticism is directed towards the traditional procedure whereby the **strength** of *reinforced concrete (RC) walls*, serving as the lateral load resisting system of building structures, is assigned on the basis of stiffnesses that are proportional to the moment of inertia of the uncracked concrete section I_c:

$$F_i = F_0 (k_i/\Sigma k) \qquad (1)$$

in which F_i = strength assigned to wall i, F_0 = design base shear, k_i = lateral stiffness of the element and Σk = total stiffness of the resisting system. As is known, this formula gives the **forces** (in the elastic range) on each wall when all of them are equally displaced due to the in-plane rigidity of the floor slab. It does not follow that when **strengths** are allotted to the walls by means of this formula they will all have the same displacement at yield. In fact they will not, unless their lengths are equal. This can easily be seen when basic strength of materials formulas are applied to a section:

$$\varphi_y = M_y/(EI) = f_y W/(EI)$$
$$= \alpha f_y /(\ell_w E) = \alpha \varepsilon_y / \ell_w \qquad (2a)$$

in which φ_y, M_y and f_y are respectively the curvature, moment and stress at yield, W = section modulus, E = elastic modulus, ℓ_w = wall length, ε_y = yield strain and α = $\ell_w W/I$. For a symmetric homogeneous section α = 2. However, for bilinear approximation the plastic moment M_p, which is larger, is used, so that $\alpha > 2$. For cracked rectangular RC wall sections in flexure, or with some axial forces due to gravity, and having practical distributions of longitudinal reinforcement $\alpha \approx 2$ [2, 3]. Equation 2a can therefore be rewritten as:

$$\varphi_y = 2\varepsilon_y / \ell_w \qquad (2b)$$

It is thus clear that yield curvature is inversely proportional to wall length. It follows that under translational motion of the structure the longest wall yields first, and thus has the largest ductility demand; i.e. the walls cannot all yield simultaneously, as predicted by Eqn.1 unless they have the same lengths. From the above it also follows that stiffness and strength are interdependent, as is obvious to designers of steel structures. Yet, since the effective moment of inertia I_e of the member used in structural analysis is usually taken as a given fraction of the gross un-cracked I_c, i.e. the effect of the actual reinforcement ratio being ignored, designers of RC structures routinely assume that stiffness and strength are separable.

Note that the wall stiffness at base can be inferred from Equation 2, but it does not necessarily follow that it faithfully represents the stiffness along the wall height (see e.g. [4,5]). However, in this paper it is assumed that the whole wall has the same stiffness.

The facts that flexural yielding develops in cantilever walls of different lengths at different curvature levels, and that usually these form only at the lower ends of the walls, while the walls at the upper storeys remain elastic, lead to a redistribution of the lateral forces among the walls. This redistribution, which is different from the one that is usually expected, occurs in the interval between the onset of yielding of the longest and the shortest walls, and manifests itself in a transfer of shear forces through the floor diaphragms. The wall forces thus transferred can be quite large. This phenomenon, which is apparently overlooked, is the main subject matter of this paper.

[1] *Professor Emeritus, Faculty of Civil Engineering, Technion - Israel Institute of Technology, Haifa, Israel.*

[2] *Consulting Engineer, Netanya, Israel.*

Before considering the problem at hand it is important to appreciate the design implications of the strength-stiffness interdependence in flexural wall systems, and in fact in all RC structures that are designed to yield. If the engineer decides to change the strength of a given element by changing its steel ratio, this modification alters the stiffness as well. Paulay [1] and Priestley and Kowalsky [6] propose to allocate strength to the walls in proportion to ℓ_w^2 (assuming equal thickness for all walls), which is the strength proportionality for rectangular walls with similar reinforcement and axial stress ratios. The response of the structure is then evaluated on the basis of this assumption.

LATERAL LOAD DISTRIBUTION

Consider first a one-storey structure laterally supported by a number of ductile structural elements, say, simple cantilevers, that are all connected to a rigid roof diaphragm. Assume that, because of their different lengths, the yield displacements of the cantilevers are different. At a certain level of the lateral load the longer wall yields, but with increasing lateral loading this wall will normally continue to carry the moments and shear forces it has accumulated up to the brink of yield. If it is also assumed that the cantilevers are elastic-perfectly-plastic, then, with increasing lateral loading on the structure as a whole, no additional forces will be taken by this element. In other words the added lateral loading will be redistributed among the remaining – so far elastic – elements. An example of this well understood behaviour is given in Paulay and Restrepo [7], and the resulting force-displacement relationship shown in their paper is reproduced in Figure 1.

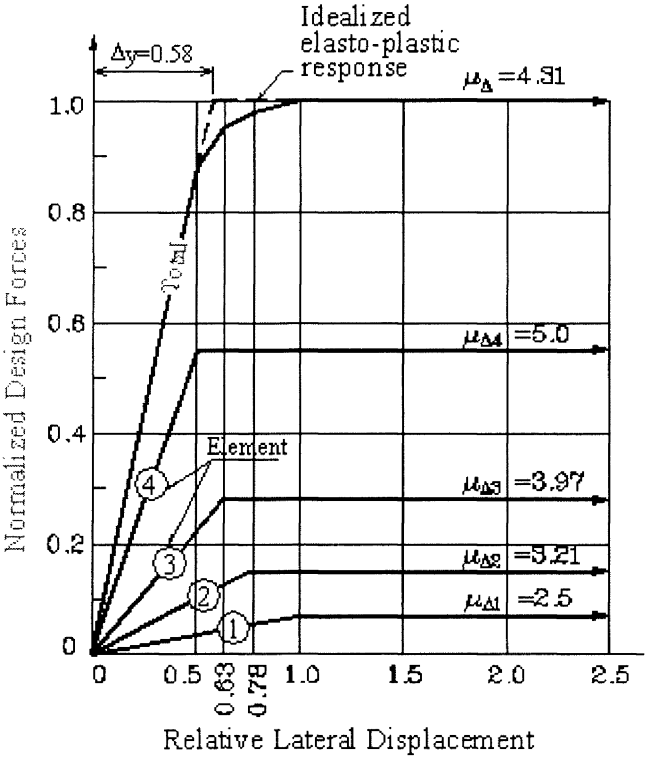

Figure 1. Force – displacement relationship for a system of one-storey walls having equal roof displacements [7].

However, in multistorey buildings with rigid floor diaphragms the behaviour of similar cantilevers will be different since the distribution of the lateral loading added after first yield will not be the same. Whereas, as expected, the moment acting at the base of the yielded wall will remain unchanged, or will increase slowly depending on the secondary slope ratio, the shear forces acting on its first storey will change sign, thereby increasing the shear forces acting on the remaining elastic walls. As a result the total shear forces acting on these walls will be larger than predicted by the conventional redistribution described above. The following simple linear model illustrates the mechanism that actually takes place.

Consider now the two-storey system supported by two walls shown in Figure 2a. Wall A is fully fixed at its base, whereas Wall B, which is longer, is hinged. The two infinitely rigid pin-ended horizontal members model the floor slabs connecting the two walls. For simplicity assume that the external horizontal force acts only at roof level. If the hinge at the base of Wall B has formed at a horizontal force level H, an additional force ΔH in the same direction will be acting only on Wall A if Wall B deflects with Wall A without resistance. But this requires that another hinge forms in Wall B at first floor level, which is not the case. To fix ideas, let Wall B be very much stiffer than wall A. Therefore, under a force increment ΔH Wall B will enforce on Wall A its straight-line deflected shape at every floor level. The resulting forces on the system and the deflected shapes are shown in Fig. 2b, assuming simple flexural behaviour (i.e., ignoring shear deformation). It can be seen that the shear on Wall A, ΔS_A, is increased by $2.5\Delta H$ ($=1.25\ \Delta M_b/h$, ΔM_b = incremental base moment, h = storey height), and the shear on Wall B is reduced by $1.5\Delta H$. In fact, for a rigid Wall B and a large number of equal storeys, it can be shown that $\Delta S_A = (3 - \sqrt{3})\Delta M_b/h$, which is quite close to the two storeys value. For the more realistic case when Wall B is 4 times stiffer than Wall A and for inverted triangular load distribution $\Delta S_A = 1.05\Delta M_b/h$ for an 8-storey model. The latter value will become handy subsequently in the numerical example. Note that, whereas the shear force increments on the walls are proportional to ΔM_b, they are not proportional to their respective total base moments.

In an elastic-perfectly-plastic system all this takes place without a change in the hinge moment because the sense of curvature remains the same. Real systems are, of course, much more complicated than that: they are unlikely to be fully fixed at the foundation level and shear deformations may become important. Also, the assumption of concentrated plasticity is a very crude approximation for walls of some depth, the hinge lengths will increase with increasing ΔH, and the transition of the force-displacement curve to the secondary slope is not abrupt, as assumed in this model. Therefore, in many instances this effect can be much less pronounced than in this case, also because Wall B is not necessarily very much stiffer than Wall A. Yet, this simple model does show that the shear forces acting on the shorter wall may be larger than those evaluated on the basis on the usual assumptions. In other words, it may not be correct to assume, as usually is done in practice, that shear force demand is proportional to bending moment demand.

Now assume that the moment-curvature relation is bilinear, so that the individual walls in the system can resist some additional loading after yield. In this case the system in

Figure 2 will remain stable also after Wall A yields. With increasing lateral loading the stiffer Wall B will increase its share in the shear. The extent of this recovery will depend, inter alia, on the relative secondary slope ratios of the two walls, and, of course, on the available ductility. In the following section two numerical examples are presented to illustrate the points made so far.

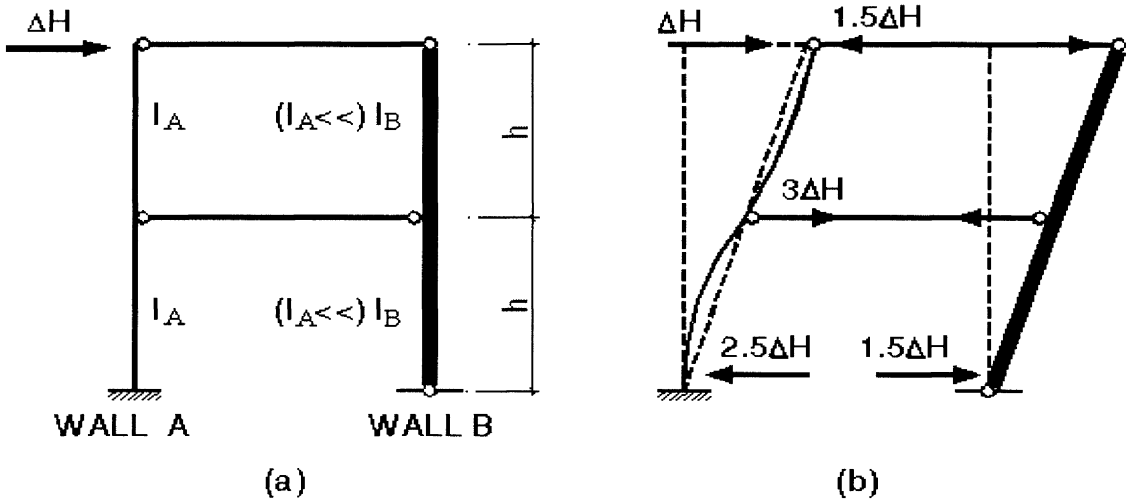

Figure 2. Two-storey wall system: (a) Properties and loading. (b) Floor forces, base shears and deflected shapes.

NUMERICAL EXAMPLES

Two numerical examples are presented. Both of them relate to the 8-storey building on rigid foundation studied extensively by Priestley and Kowalsky [6]. The plan and elevation of their building are shown in Figure 3. The wall elements were modelled as one-component Giberson beams, and their moment-curvature relations were assumed to be bilinear, with secondary slope ratios of 1.5% of the elastic one for the short wall and 1.9% for the long wall (Kowalsky [8]). Plastic hinges were allowed to extend to the full length of the first storey, as suggested by Kowalsky [8]. Note, however, that hinges were also allowed to develop in the upper storeys.

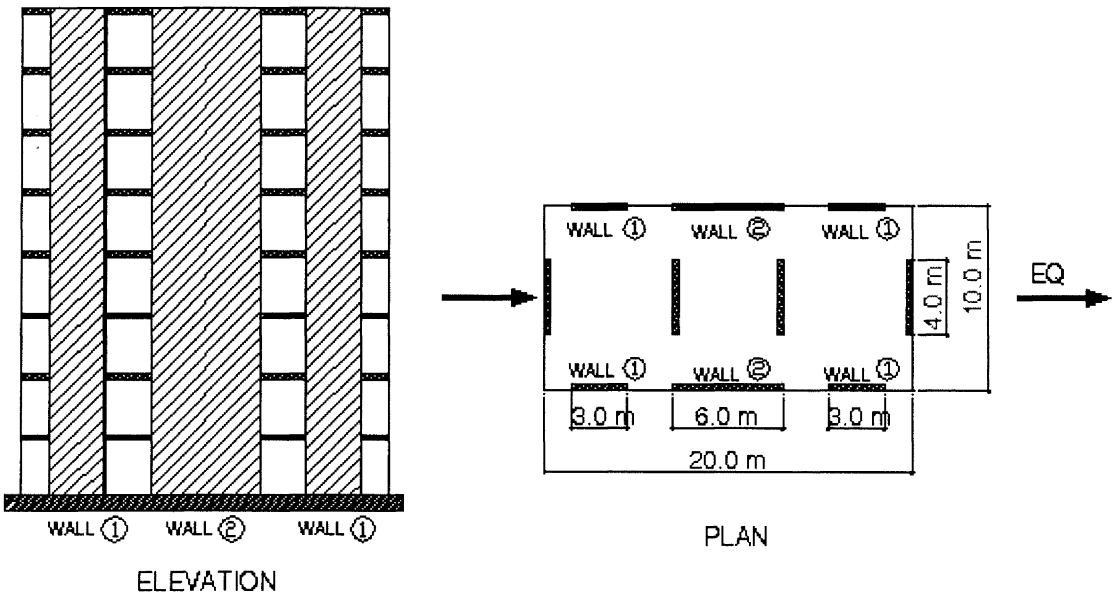

Figure 3. Plan of 8-storey wall-supported building [6].

The first example gives the results of two pushover analyses with inverted triangular loading pattern for two alternative strength-to-stiffness relationships. In the first model, which is the one used by Priestley and Kowalsky, strength is proportional to ℓ_w^2. In the second model, which is sometimes adopted by engineers and researchers, strength is ℓ_w^3 - proportional, i.e., strength is allotted per Equation 1. The pushover and inelastic time-history analyses were performed using the 2-dimentional option of the computer program RUAUMOKO [9]. This program treats pushover analysis as a dynamic problem. Hence care must be exercised to minimize the inertial effects. Therefore some minor modifications in the data file [8] were made.

Figure 4 shows the base shear vs. roof displacement Δ for each of the two walls when acting as independent structures. It can be seen that the strength of the short walls (Wall 1) is approximately one quarter of that of the long wall (Wall 2), but their yield displacement is twice as large, as predicted by Equation. 2. Figure 5 presents the base shear distributions among the walls vs. roof displacement for the two alternatives of strength to stiffness relationship. Note that only half of the structure was modelled, and it consists of **two** short walls (denoted 2 x Wall 1) and **one** long wall. The difference between the two responses after first yield is immediately apparent. Whereas the base shear partition between the walls with the ℓ_w^3-proportional strengths (Fig. 5b) is quite regular, substantial load redistribution is predicted for the ℓ_w^2-proportional model (Fig. 5a). This can better be seen in Figure 6 in which the relative share of the base shear resisted by each wall is shown. Note the large shear force transfer from the long wall to the short ones at roof displacement $\Delta \cong 100$ mm (base shear $\cong$ 1,000 kN), which occurs when the first plastic hinge is formed at the bottom of Wall 2 (Figs. 5a and 6a). It is evident that the effect is due to the presence of the walls in the upper storeys that remain elastic and are constrained by the floors to move in unison. This behaviour is not predicted by the ℓ_w^3-proportioning (Figs. 5b and 6b).

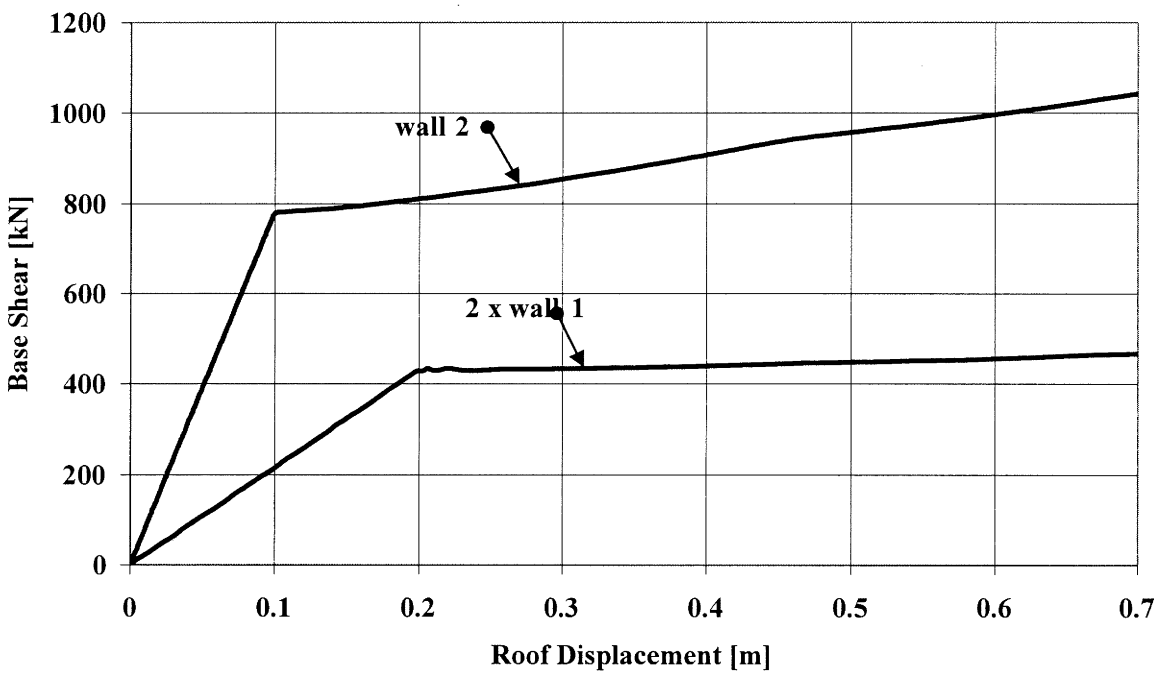

Figure 4. Force - displacement curves for each of the two walls.

It may be interesting to trace the plastic hinge formation sequence with increasing loading. At $\Delta \cong 120$ mm another hinge is formed in Wall 2 at the top of the first storey. At $\Delta \cong$ 140 mm hinges are formed at the bottom of the short walls, and at this point the roles of the two walls are reversed: Walls 1, which now have a plastic hinge at their lower end, are unloading their shear to Wall 2, which, with bottom and top hinges behaves as a fixed-base wall, albeit only with its post-yield stiffness. At a much larger roof displacement top hinges are formed also in Walls 1. Note that at these large displacement levels the shear force distributions among the walls are quite similar for the two strength assumptions (compare Fig. 5a with 5b). This is expected since after the two first storey walls have yielded bottom and top, the load is divided between them in proportion to their secondary slopes, provided these are very small relative to their primary ones. The most important effect of load redistribution among the walls is the fact that the maximum shear force acting on the short wall is larger than commensurate with its peak moment. This effect should be distinguished from shear amplification due to higher modes, which will be referred to subsequently. Therefore, conventional capacity design practice may not capture this phenomenon. Note that the plots are extended to Δ = 700 mm. This has been done to show the trends, and does not imply that the walls possess the ductility capacity consistent with this roof displacement.

Figure 7 shows the base moment distribution among the walls vs. roof displacement for the two models. It is seen that

after yield of the longer wall the ℓ_w^2-proportional strength model (Fig. 7a) predicts substantial moment redistribution compared with the response of the conventional model shown in Fig.7b. Figure 8 shows the relative share of the base moment resisted by each wall for the ℓ_w^2-proportional strength model. The ℓ_w^3-proportioning leads to flat shapes similar to those for the base shear shown in Fig. 6b.

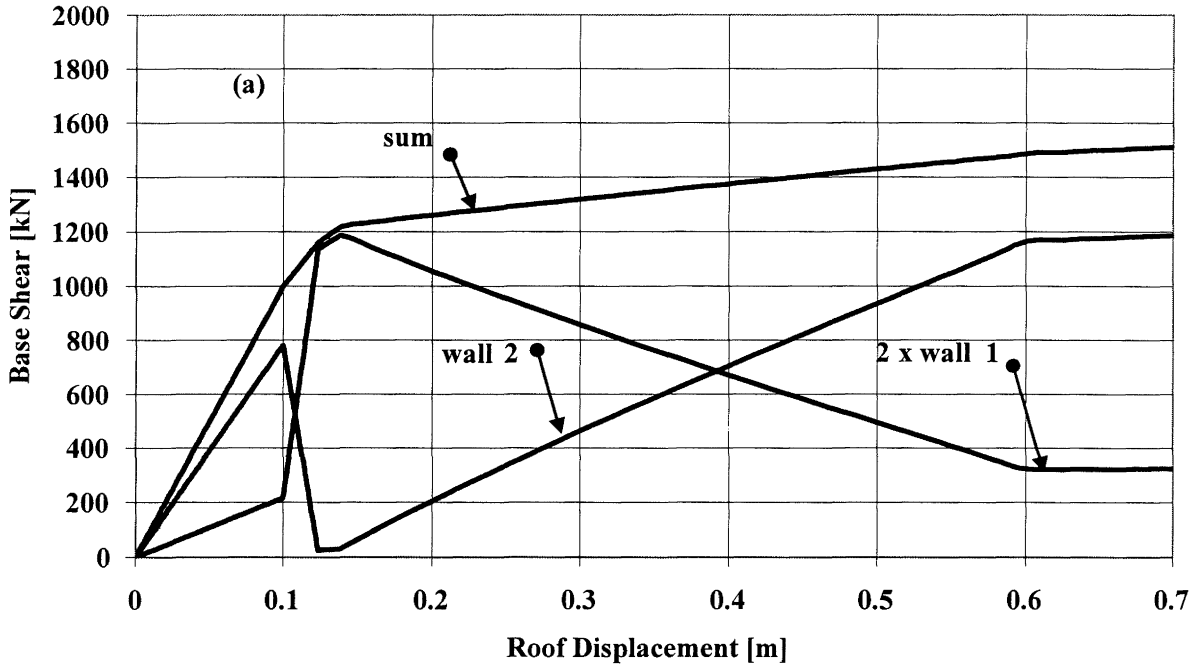

Figure 5a. Base shear vs. roof displacement: "ℓ_w^2-proportional" strength.

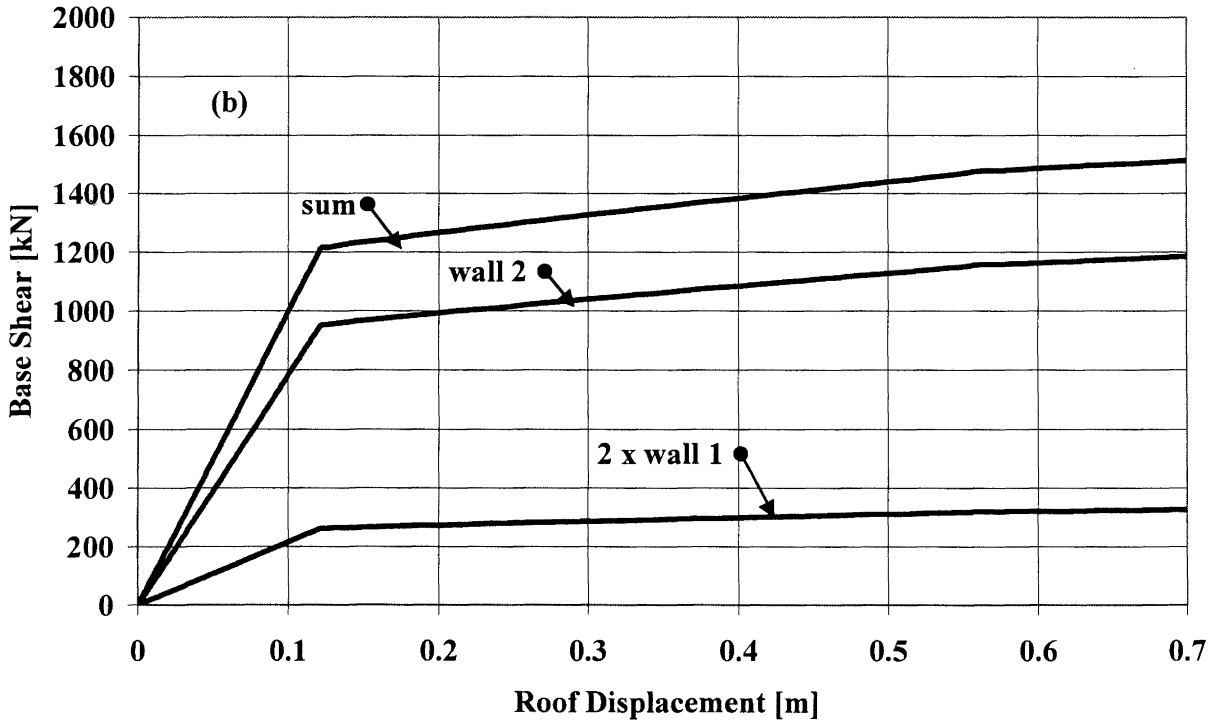

Figure 5b. Base shear vs. roof displacement: "ℓ_w^3-proportional" strength.

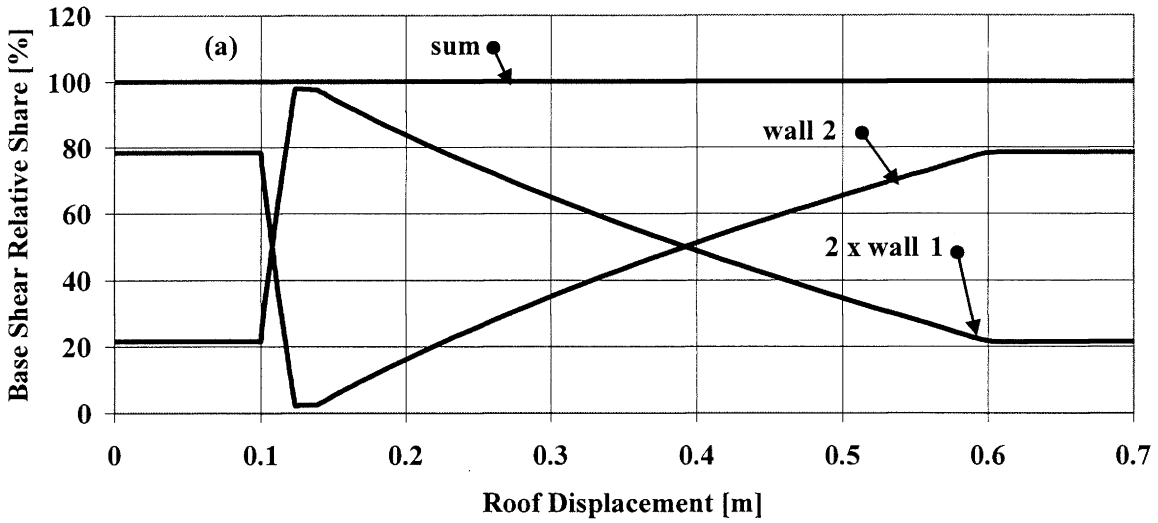

Figure 6a. Relative share of base shear vs. roof displacement: "ℓ_w^2 -proportional" strength.

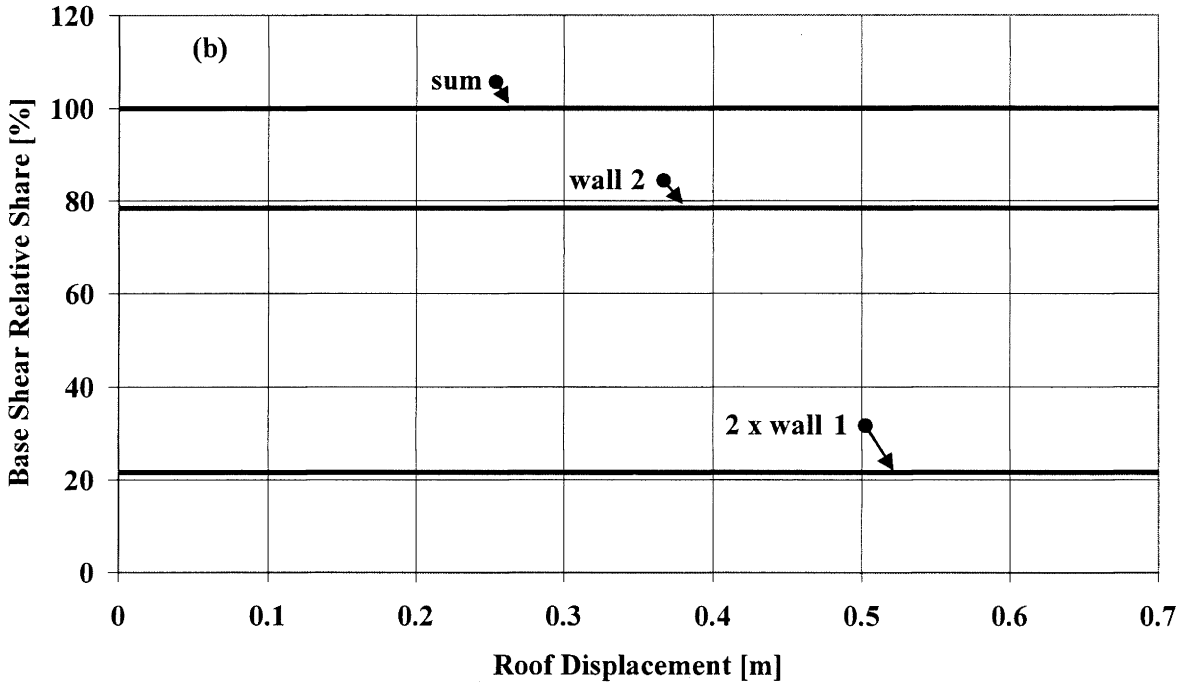

Figure 6b. Relative share of base shear vs. roof displacement: "ℓ_w^3 -proportional" strength.

Another important effect is the large in-plane forces acting on the floor slabs at the two levels above ground after first yield, as shown in Figure 9. The couples formed by these forces are the mechanism through which the moments and shear forces are transferred from wall to wall. Note that since in the pushover analysis the lateral forces were allotted to the walls in proportion to their stiffness, the floor slab forces in the ℓ_w^3-proportional model are by definition equal to zero.

It has been suggested [10] that better insight into this somewhat unexpected behaviour of the system could be gained by suppressing the formation of plastic hinges at the

top of the ground storey walls and at the bottom of the second storey. The results in Figures 10, 11 and 12 show that the differences between the responses of the two models are in the distribution of the base shear and floor slab forces at larger displacement levels, while the moment distribution is very little affected. Also, the suppression of the top hinge of the stiffer wall leads to a substantial increase in the shear demand on the flexible walls.

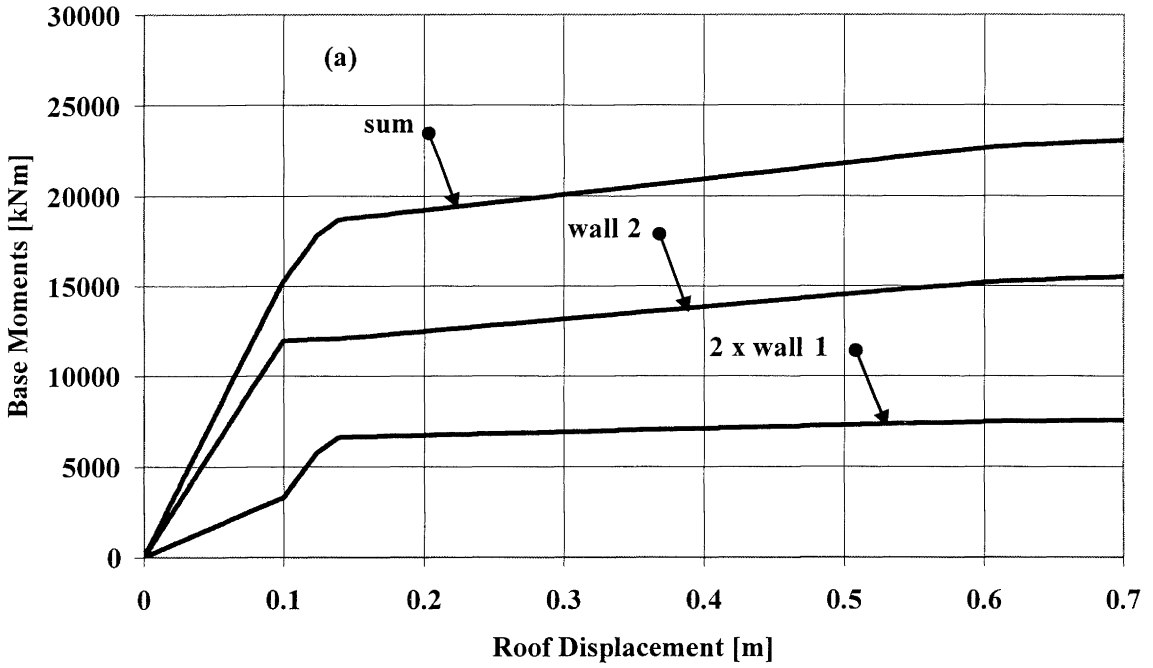

Figure 7a. Base moment vs. roof displacement: "ℓ_w^2 -proportional" strength.

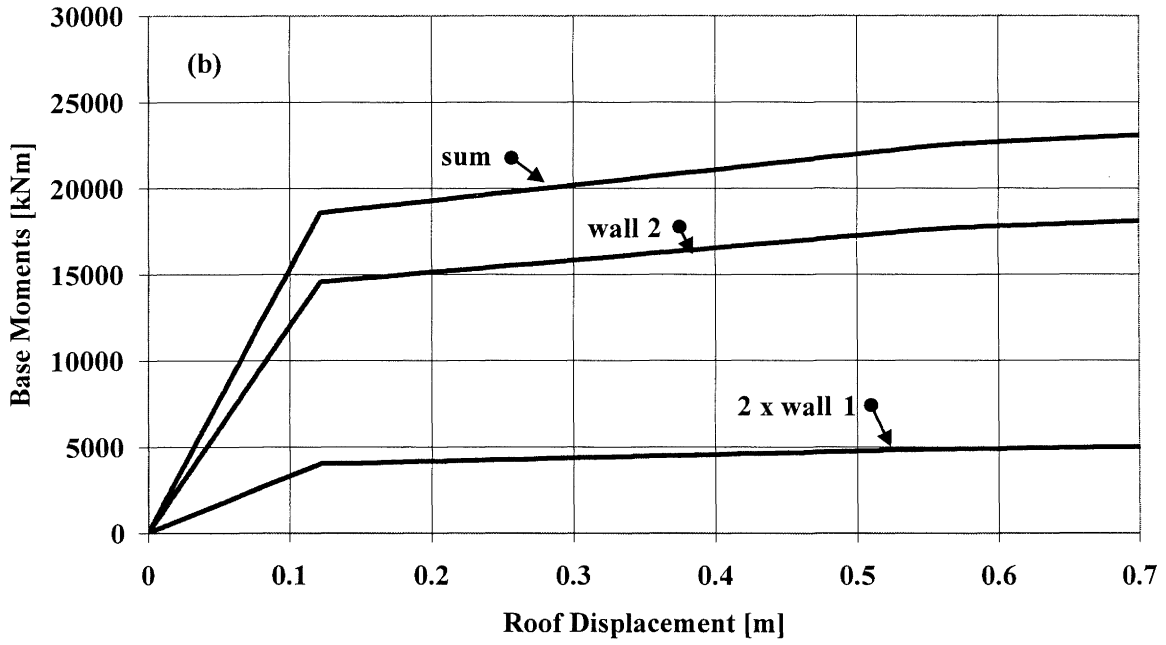

Figure 7b. Base moment vs. roof displacement: "ℓ_w^3 -proportional" strength.

It may also be interesting to note that when shear deformations in the walls were considered (30% of the concrete shear rigidity in the lower two storeys and 100% thereof in the upper storeys) the results remained practically unchanged.

The second example presents results of a series of time history analyses performed on the same rigid base model (ℓ_w^2-proportional strength) with the 5 artificial accelerograms used by Priestley and Kowalsky [6] in their verification studies. Peak ground acceleration was

normalized to 0.32g, i.e., corresponding to the NZS 4203 [10] zone factor Z = 0.8. The walls were modelled as Modified Takeda degrading stiffness elements, assuming unloading stiffness ratio of $\mu^{-0.5}$ (μ = ductility ratio at load reversal) [8]. 1.6% damping in the 1st and 2nd mode was assumed as in ref. 6. Note that this choice may lead to significant damping moments at the plastic hinges due to the resulting over-damping of higher modes [9]. Table 1 compares the mean values of the peak wall moments and shear forces at the base with their counterparts as given in ref. 6, or inferred from the results therein. It can be seen that, whereas the moments are in satisfactory agreement, the base shears differ, and are much larger than predicted in ref. 6, particularly in the short walls. This shows that the shear transfer from the long to the short walls should be taken into account, but also that, as is known, the base shear is strongly affected by the higher modes of vibration, i.e. that the effective height of the horizontal force resultant is much lower than predicted on the basis of the first mode approximation, with dynamic shear magnifications on the order of two being quite common. This effect was quantified many years ago by the New Zealand Concrete Code [12] through a dynamic shear magnification factor ω_v based on the work of Blakeley *et al* [13]. Later studies (e.g. [14]) confirmed in general that approach. Note also that the total base shear in Table 1 is smaller than the sum of the peak shear forces V_{ui} in the walls because they are not simultaneous.

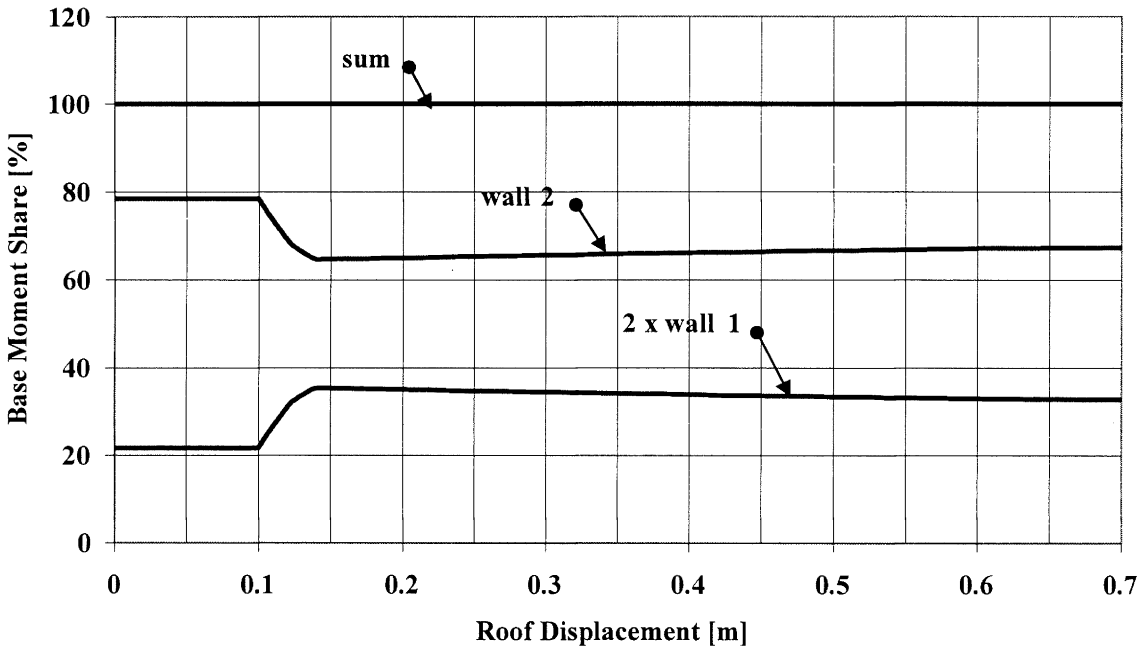

Figure 8. Relative share of base moment vs. roof displacement for "ℓ_w^2-proportional" strength.

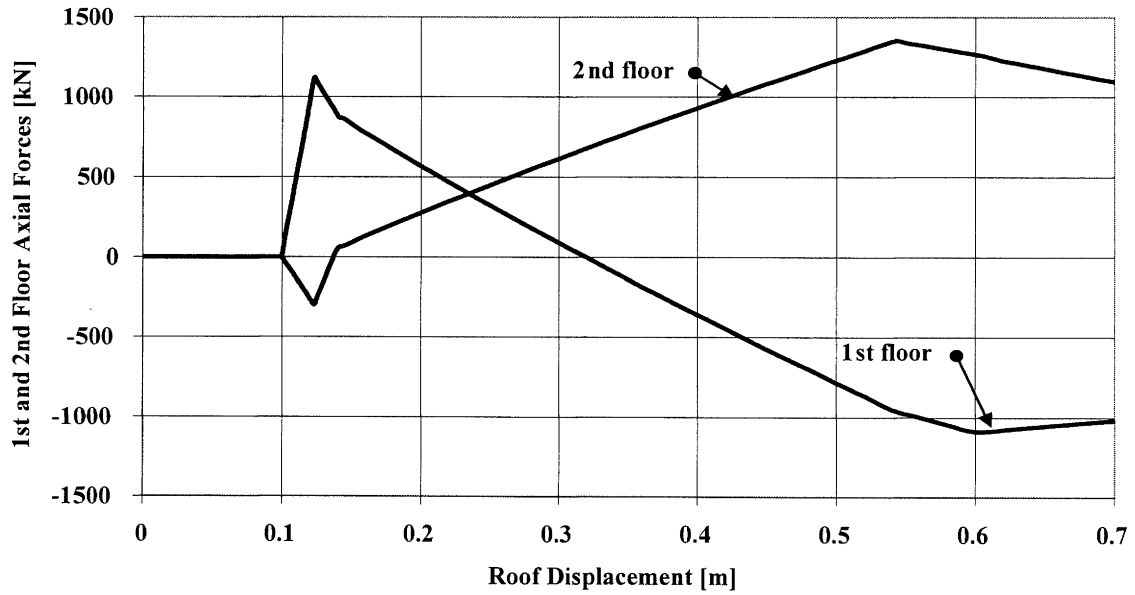

Figure 9. First and 2nd floor in-plane forces vs. roof displacement for "ℓ_w^2-proportional" strength.

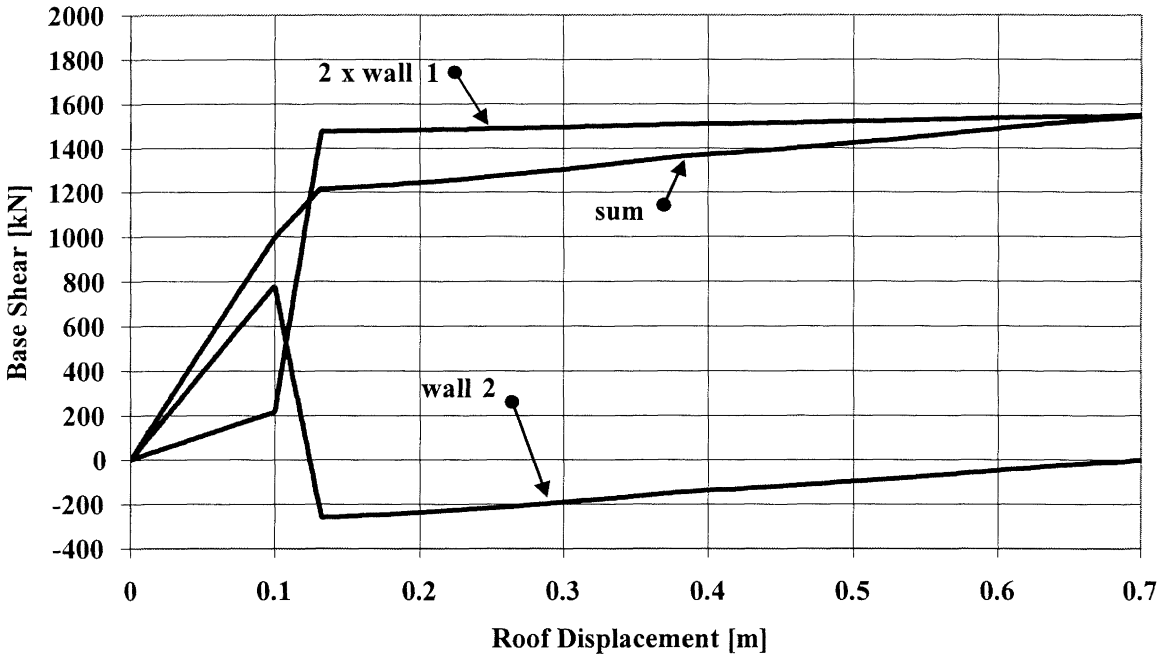

Figure 10. Base shear vs. roof displacement for [3] ℓ_w^2 – proportional" strength – plastic hinges only at base.

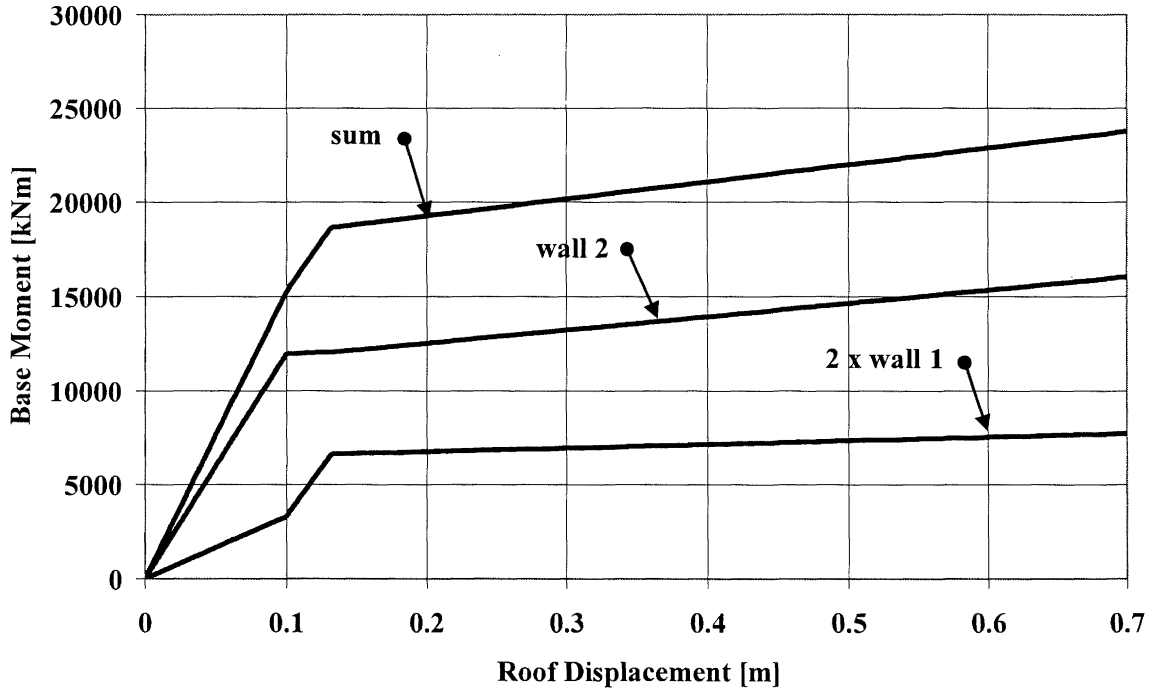

Figure 11. Base moment vs. roof displacement for "ℓ_w^2 -proportional" strength – plastic hinges only at base.

A crude estimate of the shear demand on the walls can be obtained as follows. If it is assumed that due to higher modes effects the base shear is twice that computed from the inverted triangular distribution leading to flexural yield (which in this case was found to be an underestimate), the following values for the base shears V: V_{1y} = 2 x 216/ 2 = 216 kN; V_{y2} = 2 x 775 = 1,550 kN (at $\Delta \cong$ 0.1m in Fig. 5a) are obtained. The latter value should be compared with 1,923 kN in Table 1. The base shear transferred to the short walls after yield of the long walls can be estimated by noting that the additional moment ΔM that the system can carry after Walls 2 have yielded $\cong$ 6,600 kNm ($\cong$ the residual capacities of Walls 1). Noting that in the static analysis the additional shear ΔH on the 4 Walls 1 (for wall stiffness ratio $\cong$ 3.6) $\cong$ 1.0 x $\Delta M_b/h$ = 6,600/ 2.7 $\cong$ 2,440 kN, or 610 kN on each wall, the peak base shear on Wall 1 $\cong$ 216 + 610 = 826 kN (compare with 786 kN). Note that no allowance for strain

hardening has been made since similar peak shear values were obtained in the analyses of this structure for the same records when elastic-perfectly-plastic behaviour was assumed.

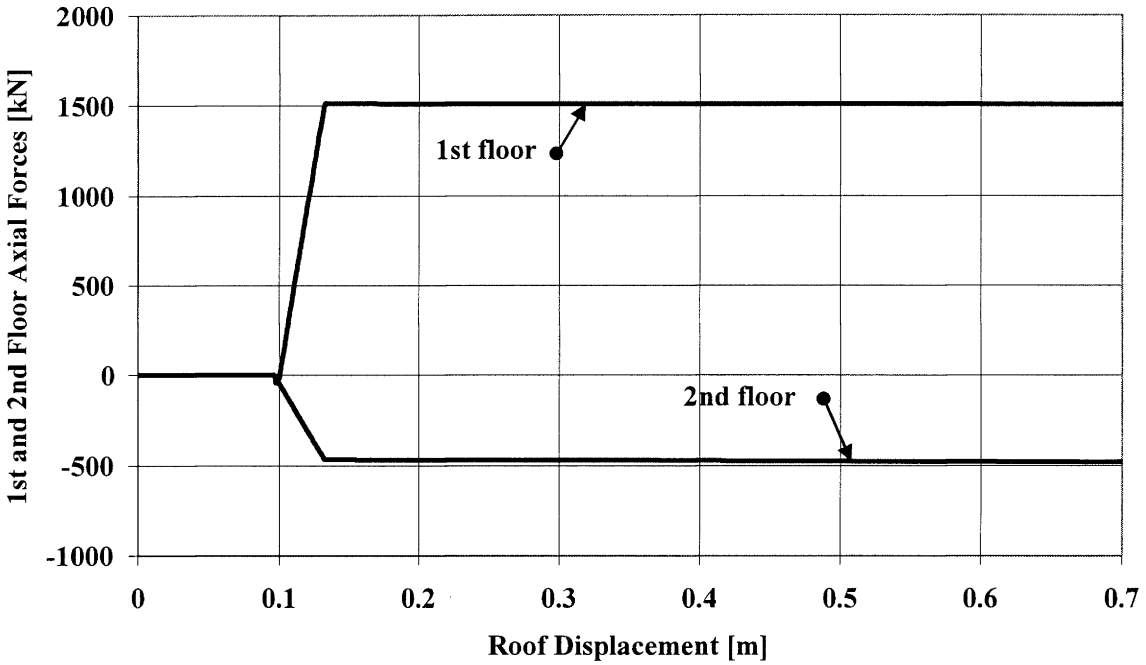

Figure 12. First and second floor in-plane forces vs. roof displacement for "ℓ_w^2 -proportional" strength – plastic hinges only at base.

The assumption that the maximum base shear in the long wall can be predicted by its value at yield, as has been done above, may lead to a gross underestimation. This is due to the fact that if full moment reversal takes place when the long wall base shear is very low (e.g., as at circa 12 sec. in Fig. 5a), or even negative, the resulting shear on it may practically double.

The base shear time-history of the two walls for the El Centro record, normalized to 0.32g, is shown in Figure 13. Note that the largest peaks in Walls 1 and 2 are similar in magnitude to their counterparts in Table 1 (Wall 1 shear force in Fig. 13 should be divided by 2). The time history of the roof displacement is given in Figure 14, with a peak value of 0.23 m. RUAUMOKO predicts peak curvature ductility demands of circa 2.5 for Wall 1 and 4.0 for Wall 2.

SUMMARY AND CONCLUSIONS

The results of the analyses show that conventional modelling, i.e., basing stiffness of RC elements on their gross moment of inertia irrespective of their steel content may underestimate the maximum shear forces acting on the shorter walls in structures having shear walls of different lengths. Furthermore, even a more realistic strength allocation among the walls may lead to erroneous conclusions if the effect of the predominantly elastic walls in the upper storeys is not accounted for. Therefore, caution should be exercised when using a one-storey "equivalent" model for multistorey reinforced concrete wall systems. In other words: whereas the wall moments can be estimated from the analysis proposed in ref. 6, the evaluation of the shear demand should consider the restraining effect of the upper storeys that mostly do not yield, as well as the effects of higher modes of vibration. Finally, appreciable in-plane forces are likely to develop in the 1st and 2nd floor slabs, and these should be considered in the design.

The pushover results presented in this study were compared with results based on different modeling assumptions, such as rounded, rather than abrupt, transitions from the linear to the yielding regions of the moment-curvature relationships, the introduction of four beam elements in the first storey to better simulate progressive yielding, and accounting for shear deformations (which were deliberately suppressed in the reported results to allow comparison with [6]). Yet, no material differences were observed in the shapes of the response curves. This should not be very surprising to those familiar with the behaviour of wall structures in which some of the walls are hinged at base level (e.g. [15]). The difference lies in the fact that herein the hinge is plastic, whereas in that study and earlier ones the hinge was preformed.

ACKNOWLEDGEMENTS

The authors are indebted to Prof. M.J. Kowalsky for providing the RUAUMOKO input data files, the suite of accelerograms for the 2nd example, and the clarifications regarding modelling. The first author is also indebted to Prof. J. Restrepo for fruitful discussions and for his insightful suggestions. The useful suggestions of the anonymous reviewer are gratefully acknowledged. This work was supported by the Fund for the Promotion of Research at the Technion.

Table 1: Comparison of results with Priestley & Kowalsky [6]

	A (m^2)	EI (kNm^2)	My (kNm)	Mu (kNm) P&K	Mu (kNm) R&L	Vu (kN) P&K	Vu (kN) R&L
Wall 1	0.75	$2.2x10^6$	3,307	3,516	3,492	221	786
Wall 2	1.50	$15.95x10^6$	11,956	14,064	13,445	882	1,923
Total *	6.00	$40.7x10^6$	37,140	42,192	40,858	2,647	5,896♦

NOTES: P&K – Priestley & Kowalsky. R&L – present study. * 4 x Wall 1 + 2 x Wall 2. ♦ Base shear

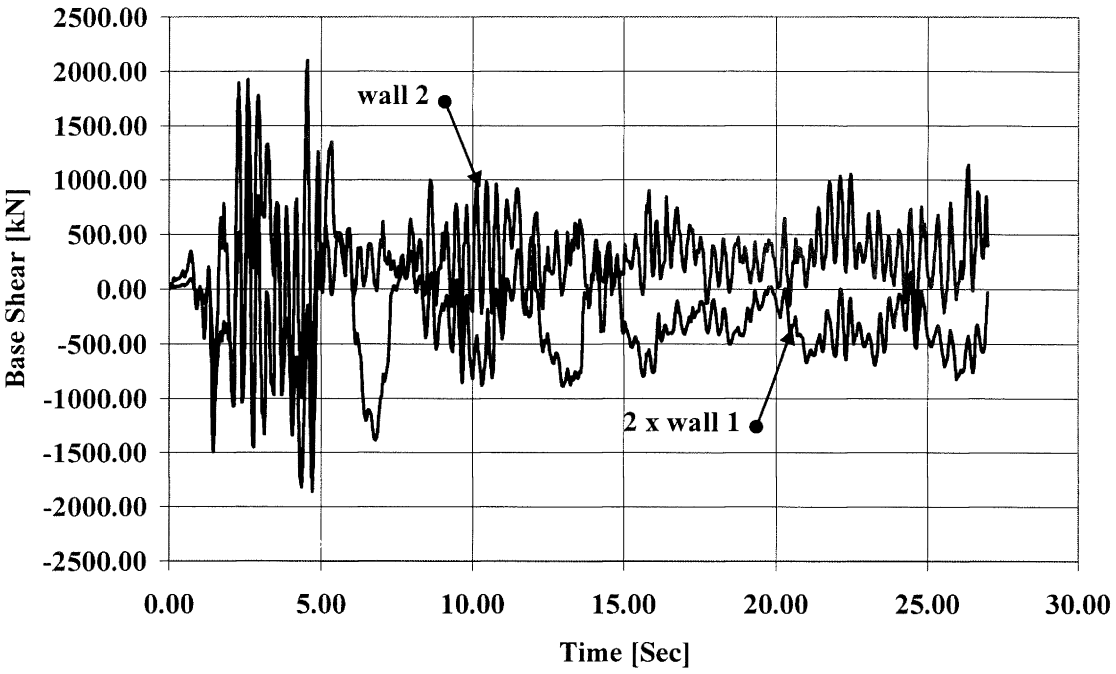

Figure 13. Base shear time-history for the 1940 NS component of the 1940 El Centro record.

REFERENCES

1. Paulay, T. (1997). "Seismic torsional effects on ductile structural wall systems". *J. Earthq. Engng.* **1** (4), 721-745.

2. Paulay, T. (1999). "Some principles relevant to the seismic torsional response of ductile buildings". Proceedings, 2nd European Workshop on Irregular and Complex Structures, Istanbul, Oct. 1999.

3. Priestley, M.J.N. (1997). "Displacement-based seismic assessment of reinforced concrete buildings. *J. Earthq. Engng.* **1** (1), 157-192.

4. Fenwick, R. and Bull, D. (2000). "What is the stiffness of reinforced concrete walls?". *J. New Zealand Structural Engng. Soc.* **13** (2), 23-32. Discussion: Priestley, M.J.N. & Paulay, T. (2000), **15** (1), 30-34, Response: 35-41.

5. Fenwick, R., Hunt, R. and Bull, D. (2001). "Stiffness of structural walls for seismic design". *J. New Zealand Structural Engng. Soc.* **14** (2), 22-34.

6. Priestley, M.J.N. and Kowalsky, M.J. (2000). "Direct displacement-based seismic design of concrete buildings". *Bull. New Zealand Natl. Soc. Earthq. Engng.* **33** (4), 421-444.

7. Paulay, T. and Restrepo, J. (1998). "Displacement and ductility compatibility in buildings with mixed structural systems". *J. New Zealand Structural Engng. Soc.* **11** (1), 7-12.

8. Kowalsky, M.J. (2001). Personal communication.

9. Carr, A.J. (2000) "RUAUMOKO – Program for inelastic dynamic analysis", & Manual. Department of Civil Engineering, University of Canterbury, Christchurch.

10. Restrepo, J. (2001). Personal communication.

11. New Zealand Standards Association. (1992). "NZS 4203: Code of practice for general structural design and design loadings for buildings", Wellington.

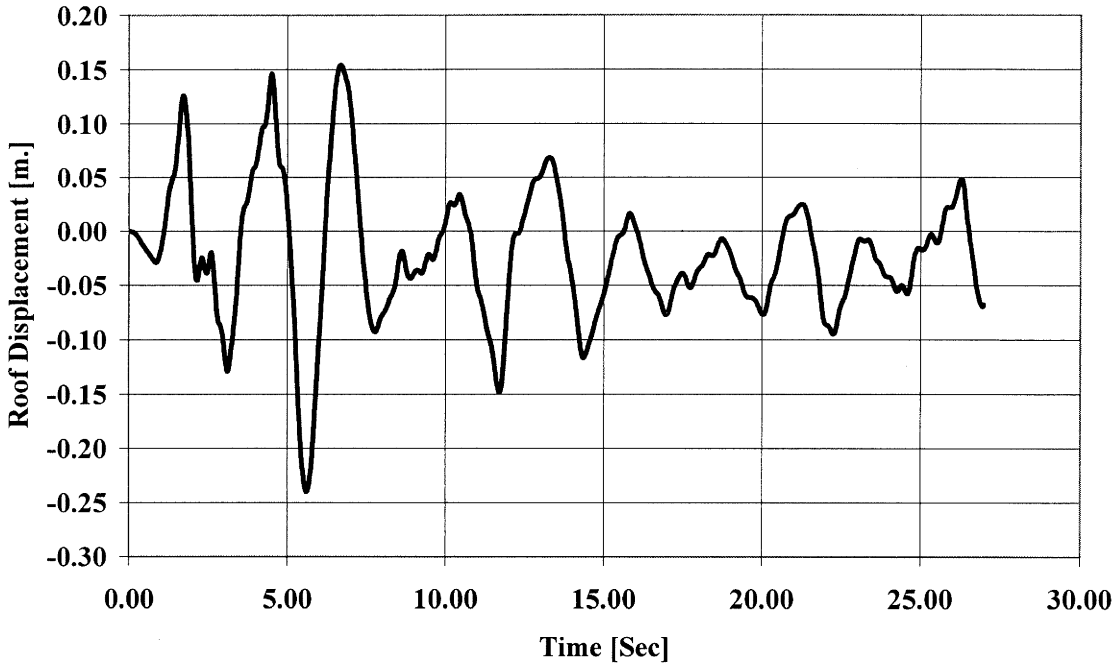

Figure 14. Roof displacement time-history for the 1940 NS component of the 1940 El Centro record.

12. New Zealand Standards Association. (1995). "NZS 3101: Concrete Structures Standard (Parts 1 & 2)", Wellington.

13. Blakeley, R.W.G., Cooney, R.C. and Megget, L.M. (1975). "Seismic shear loading at flexural capacity in cantilever wall structures". *Bull. of the New Zealand Natl. Society for Earthq. Engng.*, **8** (4), 278-290.

14. Filiatrault, A., D'Aronco, D. and Tinawi, R. (1994). "Seismic shear demand of ductile cantilever walls: a Canadian perspective". *Canadian J. of Civil Engng,*, **21**, 363-376.

15. Paulay, T. and Priestley, M.J.N. (1992). "*Seismic Design of Reinforced Concrete and Masonry Buildings*", Wiley, New York (pp. 506-508).